Breast Boundary Detection With Active Contours

I. Balic[§], P. Goyal[§], O. Roy[†‡], and N. Duric[†‡]

§ Sonoview Acoustic Sensing Technologies,
EPFL Innovation Park, Bâtiment I,
1015 Lausanne, Switzerland

† Delphinus Medical Technologies,
46701 Commerce Center Drive,
Plymouth, MI 48170, USA

‡ Karmanos Cancer Institute,
4100 John R,
Detroit, MI 48201, USA

ABSTRACT

Ultrasound tomography is a modality that can be used to image various characteristics of the breast, such as sound speed, attenuation, and reflectivity. In the considered setup, the breast is immersed in water and scanned along the coronal axis from the chest wall to the nipple region. To improve image visualization, it is desirable to remove the water background. To this end, the 3D boundary of the breast must be accurately estimated. We present an iterative algorithm based on active contours that automatically detects the boundary of a breast using a 3D stack of attenuation images obtained from an ultrasound tomography scanner. We build upon an existing method to design an algorithm that is fast, fully automated, and reliable. We demonstrate the effectiveness of the proposed technique using clinical data sets.

Keywords: Active contours, breast boundary detection, image segmentation, ultrasound tomography

1. INTRODUCTION

Ultrasound tomography (UST) is a technique that uses computed tomography methods to solve an inverse problem involving ultrasound signals. In the scenario of interest, the breast to be imaged is immersed in a water tank, and is surrounded by an ultrasound transducer ring that moves from the chest wall to the nipple region using a motorized gantry. Each transducer element emits, in turn, an ultrasound pulse that propagates through the medium and gets recorded by all the elements of the ring aperture. Acoustic properties of the medium are inferred from the recorded ultrasound data using image reconstruction algorithms. A number of investigators have developed scanners based on UST principles. Examples include the work by Marmarelis *et al.*,[1] Johnson *et al.*,[2] Ruiter *et al.*,[3,4] and Andre *et al.*[5] Our group at the Karmanos Cancer Institute (KCI) has also focused on the development of a UST research prototype for breast cancer detection.[6] The clinical feedback obtained from the studies performed over the past decade at KCI's breast center has guided the continuous development of that prototype, as well as its upgrade to SoftVue (see Figure 1), the commercial system developed by our start-up company, Delphinus Medical Technologies. SoftVue uses tomographic reconstruction algorithms to compute a stack of reflection images, as well as quantitative information such as sound speed and attenuation of breast tissue.

Further author information: (Send correspondence to I. Balic)
I. Balic - email: ivana.balic@sono-view.com
P. Goyal - email: pulkit.goyal@sono-view.com
O. Roy - email: oroy@delphinusmt.com
N. Duric - email: nduric@delphinusmt.com

Medical Imaging 2014: Ultrasonic Imaging and Tomography, edited by Johan G. Bosch,
Marvin M. Doyley, Proc. of SPIE Vol. 9040, 90400D · © 2014 SPIE
CCC code: 1605-7422/14/$18 · doi: 10.1117/12.2043414

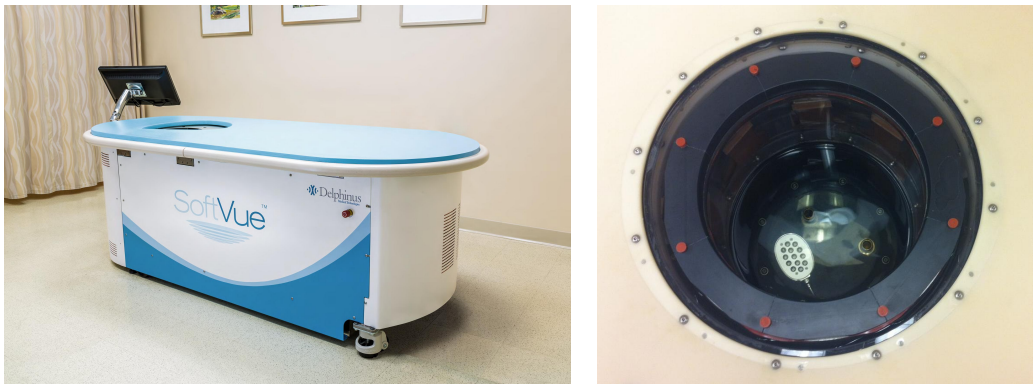

(a) (b)

Figure 1. The SoftVue scanner. (a) The table and the control display. (b) The imaging chamber and the transducer ring (top view). The breast is immersed in the imaging chamber filled with warm water and the transducer ring scans the breast along the coronal axis from the chest wall to the nipple region.

In order to optimize the visualization of these data sets on a workstation, it is useful to blank out the water region surrounding the breast since it does not contain any useful diagnostic information. Our goal is thus to design a computerized method that automatically segments out the breast from its water background. The method shall output a binary mask of the voxels inside the breast. This mask can also be used to compute statistical quantities, such as the average sound speed for breast density evaluation.[7] The problem is challenging since breasts can have various forms and shapes. Moreover, the tomographic images used for breast boundary detection may have artifacts that make it difficult to detect the boundary with high accuracy, in particular in the vicinity of the chest wall and the nipple region. To be useful in a clinical setting, the method should not require user interaction, and be fast enough to be used as a post-processing step after image reconstruction.

The proposed approach is largely based on the work exposed in Refs. 8–10, which uses active contours parameterized using exponential B-spline bases. These bases allow blob-like objects (e.g., breasts) to be represented using a small number of parameters. In other words, the breast boundary can be represented accurately in 3D using a few control points. The parametric approach is appealing from a computational viewpoint in that only few parameters need be updated at each iteration of the optimization process. It is also robust since the method implicitly takes the smoothness of the boundary of interest into account. This is in contrast to schemes that directly represent the contour as a set of voxels (see, e.g., Ref. 11). A number of practical considerations are discussed in order to use the active contour scheme for breast boundary detection. In particular, we present a mirroring strategy and an initial contour that improve the accuracy of the method in the clinical setting.

The paper is organized as follows. In Section 2, we describe the used active contour method and its mathematical background. Section 3 discusses a number of practical considerations to apply the method to the problem of breast boundary detection. Segmentation results using clinical data sets are presented in Section 4. Conclusions and future directions of research are given in Section 5.

2. SPLINE BASED ACTIVE CONTOURS

2.1 Active contours

The use of deformable models in segmentation has attracted a lot of interest in recent years since they they provide the best tradeoff between flexibility and efficiency. Within this category of deformable models, active contours[8,9,11–13] (also referred to as snakes) are the most popular tools for image segmentation. In 2D, an active contour is a curve within a 2D image that evolves from an initial position towards the boundary of the object of interest. Its extension to 3D images is an evolving surface. The initial position of the active contour is usually specified by the user, or it is provided by an auxiliary detection algorithm. The evolution of the active contour is formulated as a minimization problem; the associated cost function is usually referred as *contour energy*. Active

contours have become popular because it is possible for the user to interact with them, not only when specifying its initial position, but also during the segmentation process.

2.2 Representation with exponential B-splines

The contour can be represented in various ways, e.g., using a pixel-based approach or a parametric representation. We consider a parametric representation of an active contour. This method allows us to describe an active contour as a continuous curve using a prescribed number of control points. There are many different techniques for representing continuous curves. In computer graphics, curves and surfaces are often represented using non-uniform or uniform B-spline functions and, more recently, using non-uniform rational B-splines (NURBS). NURBS have the advantage to be closed under perspective transformations. On the other hand, curve and surface parameterizations based on Fourier descriptors and uniform B-spline functions are popular in image processing due to the existence of efficient signal processing algorithms, and their invariance to affine transformations. Of these, the B-spline curves have the extra advantage of locality of control which favors a more user-friendly interaction: a change in one of the active contour points will only affect a small region of the curve or surface, hence facilitating the optimization process.

Our approach is based on the method described in Refs. 8–10 which uses exponential B-splines to represent active contours. The active contour surface is parameterized by few control points and uses as basis functions a special kind of exponential B-splines ϕ_1 and ϕ_2 investigated in Ref. 10. The authors in Ref. 9 show that the complete parametric form of the active contour $\sigma(u,v) \in \mathbb{R}^3$ can be written as

$$\sigma(u,v) = \sum_{i=0}^{m_1-1} \sum_{j=-1}^{m_2+1} c(i,j)\phi_{1,\mathrm{per}}(m_1 u - i)\phi_2(m_2 v - j), \tag{1}$$

where $\phi_{1,\mathrm{per}}(u) = \sum_{n=-\infty}^{\infty} \phi_1(u - m_1 n)$ for all $u \in \mathbb{R}$ and $c(i,j) \in \mathbb{R}^3, (i,j) \in \mathbb{Z}^2$ are the control points in 3D that define the shape of the surface. Taking into account that the surfaces are smooth and closed, certain restrictions can be applied on the coefficients that result in having $(m_1(m_2 - 1) + 4)$ free control points. For more details, we refer to Ref. 9.

The most important feature of the proposed representation is that it allows the 3D active contour to perfectly reproduce ellipsoids. Moreover, the bases have the shortest possible support given the aforementioned ellipsoid reproduction property. Because they are also refinable, they provide a good approximation of any closed surface with a blob-like topology. The optimization process is remarkably fast and good approximation can be obtained using only a few control points. The approach is appealing in that the smoothness of the object boundary is implicitly taken into account by the description of the contour as a means to increase the robustness of the boundary detection task.

2.3 Active contour energy

Active contours are driven by an energy function that determines the quality of the segmentation. The active contour energy is typically the linear combination of three terms:

The *image energy* E_{image} is responsible for guiding the active contour towards the boundary of interest. There are many strategies to define image energy and they can be categorized in two main families: edge-based methods, which use gradient information to detect contours, and region-based methods, which use statistical information to distinguish different homogeneous regions. The edge-based energy can give a good localization of the contour near the boundaries but is sensitive to noise and has a small basin of attraction, thus requiring a good initialization. On the other hand, the region-based energy has a large basin of attraction and can converge even if explicit edges are not present. However, it does not give a localization that is as good as the edge-based energy at the image boundaries. In our breast boundary detection problem, the initialization is good enough such that the edge-based method can be chosen. The energy of the image f is defined as[9]

$$E_{\mathrm{image}} = -\oiint_S \left(\nabla f \cdot \frac{\mathbf{n}}{||\mathbf{n}||} \right) \mathrm{dS},$$

where S is the closed surface determined by the contour σ defined in (1), and $\mathbf{n}$ is the normal to the surface. The above energy term promotes an edge whose normal has the same direction as the image gradient as a means to reduce the distraction created by nearby targets.[9]

The *internal energy* E_{int} ensures that the segmented region has smooth boundaries. The active contour is globally smooth since it is represented using a smooth parametric representation with a few control points. However, the representation can be locally rough if these control points accumulate locally. In that case, the internal energy causes these points to be uniformly distributed over the surface of the active contour. In the context of 2D active contours, the internal energy is represented as a linear combination of the length of the contour and the integral of the square of the curvature along the contour. The extension to 3D can be expressed as

$$E_{\text{int}} = \lambda_1 |S| + \lambda_2 \oiint_S |K|^2 \, \mathrm{dS},$$

where K is the Gaussian curvature of the surface.

The *constraint energy* E_{cons} provides a means for the user to interact with the active contour. We do not use any constrained energy term since the method needs to be automatic and, as such, does not allow any user interaction.

With the above considerations, the total energy of the contour can be written as

$$E_{\text{total}}(c) = E_{\text{image}}(c) + E_{\text{int}}(c),$$

and the optimal control points are obtained as

$$c^{\text{opt}} = \underset{c}{\operatorname{argmin}} \, E_{\text{total}}(c).$$

2.4 Fast optimization

With the chosen parametric representation, it can be shown that the computational complexity of the optimization process is dominated by the computation of the image energy. The cost can however be significantly reduced using pre-integrated images.[9] The optimization is then carried using a standard line-search method while enforcing conjugation of the successive descent directions. The algorithm stops after a convergence criterion is met.

3. BREAST BOUNDARY DETECTION

Our automatic breast boundary segmentation algorithm is based on the method explained in Section 2. Our investigation has shown that the segmentation algorithm works best when applied to the attenuation images produced by the SoftVue scanner. This is because the attenuation images exhibit the most pronounced breast boundary since the attenuation in water is essentially zero. This boundary is further amplified by the contribution of the reflections that occur at the water/breast interface. For the method to perform well for all breast shapes and sizes, a number of modifications are done to the original algorithm.

The described parametric active contours are defined on a sphere-like topology. The spline-based parametrization models ellipsoidal objects and spheres like closed surfaces. However, the stack of breast attenuation images does not represent a closed surface. In fact, while the attenuation is always high at the breast boundary, it can be very low inside the breast (e.g., due to the presence of cysts). Therefore, the coronal slices of the breast taken close to the chest wall may appear as having "holes", i.e., regions of low attenuation surrounded by boundaries of higher attenuation. A similar phenomenon may occur if the inter-slice spacing is too large, hence creating gaps between the boundaries of consecutive slices.

Another limitation is that the boundary is typically non-smooth near the chest wall due to the coronal scan configuration. Proper fitting thus requires non-smooth active contours (e.g., using a large number of control points) which decrease the robustness of the segmentation process in other regions of the breast. To address this problem, we mirror the attenuation stack with respect to the chest wall plane such that the boundary resembles

(a) (b)

Figure 2. Mirroring strategy. (a) Original attenuation image stack. The region of low attenuation in the slices near the chest wall appears as a hole. (b) Mirrored image stack. Possible holes inside the breast are hidden.

a closed blob-like surface (see Figure 2). Note that the mirroring strategy can be directly integrated within the optimization process without having to store the mirrored portion of the stack in memory.

The region of interest is also extended beyond the imaging region to avoid instabilities during the minimization process in the case where the breast touches the transducer ring. To further assist the segmentation process, we set the initial contour to have the shape of a mirrored truncated cone (see Figure 3(a)). With this initial shape, the algorithm first finds the parameterized active contour that best matches it. The result, shown in Figure 3(b), better fits the expected shape of the breast and prevents the active contour from being attracted by artifacts generated near the transducer ring.

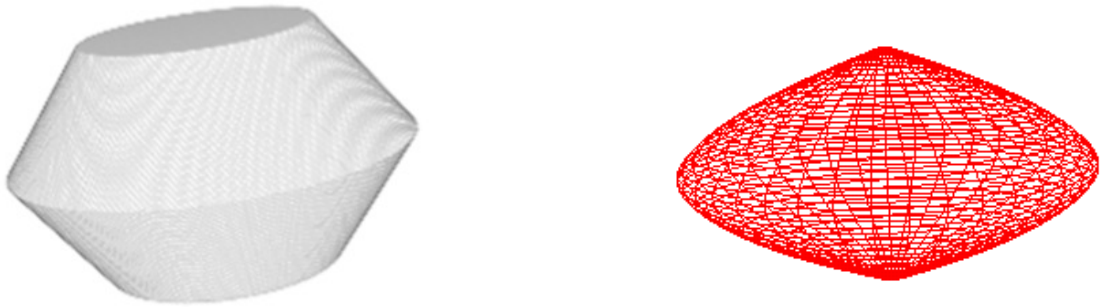

(a) (b)

Figure 3. Initial breast boundary. (a) Mirrored truncated cone used as a model for the algorithm to fit an initial parameterized active contour. (b) The parameterized active contour that best matches the mirrored truncated cone chosen as initial model.

Finally, the optimization algorithm is run iteratively on smoothed versions of the original stack. At each iteration, we decrease the smoothing factor that is applied on the stack of attenuation images. With a high smoothing factor, the active contour can see the breast boundary since the basin of attraction is increased. This allows the active contour to move from the initial estimate to a contour close to the boundary of the breast. The subsequent iterations use a decreasing smoothing factor to guide the active contour closer and closer to the actual breast boundary. In comparison to the semi-automatic algorithm proposed in Ref. 8, which requires user interaction in order to fine tune the contour, this strategy allows us to segment the breast automatically. The boundary is estimated with a good accuracy and the proposed strategy works well for different breast shapes and sizes as demonstrated in the next section.

4. RESULTS

To demonstrate the effectiveness of our approach, we present the segmentation results obtained for some attenuation stacks reconstructed using clinical data. In Figure 4, we show the segmentation of the breast obtained using the original attenuation stack without the mirroring strategy, as well as the result obtained with mirroring. We observe that the mirroring strategy builds a volume that has a closed surface hence allowing the algorithm to closely fit it. The final breast boundary is then obtained by considering only one half of the active contour (top or bottom).

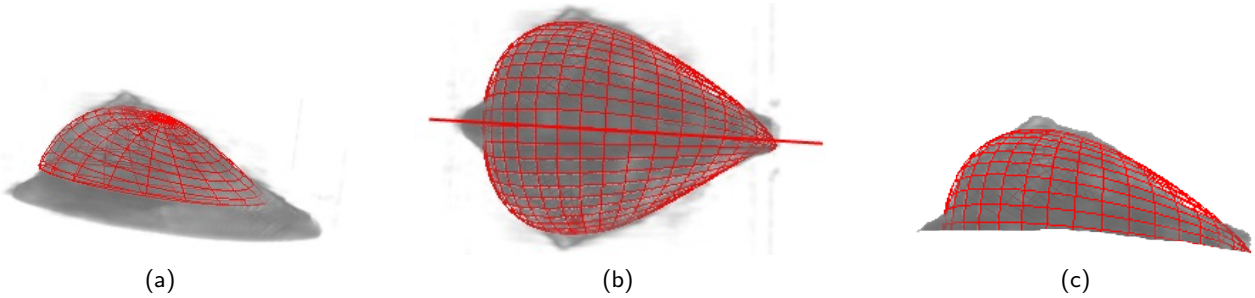

Figure 4. Breast segmentation using active contours. (a) Segmentation using the original attenuation stack. (b) Segmentation of the mirrored attenuation stack. (c) Top half of the segmented mirrored stack.

We observe that setting a good initial estimate of the contour is very important for the algorithm to converge to an accurate segmentation of the breast. In general, the algorithm works best when the initial shape encloses most of the breast. In Figure 5, we present the segmentation results obtained for two different initial shapes. The sphere shown in Figure 5(a) is too small with respect to the volume of the breast. When it is used as a starting point, the optimization algorithm does not see the boundary of the breast and fails to converge to the correct boundary. Our initial shape, shown in Figure 5(c), partially surrounds the breast allowing the algorithm to recognize the location of the breast boundary and to successfully segment it.

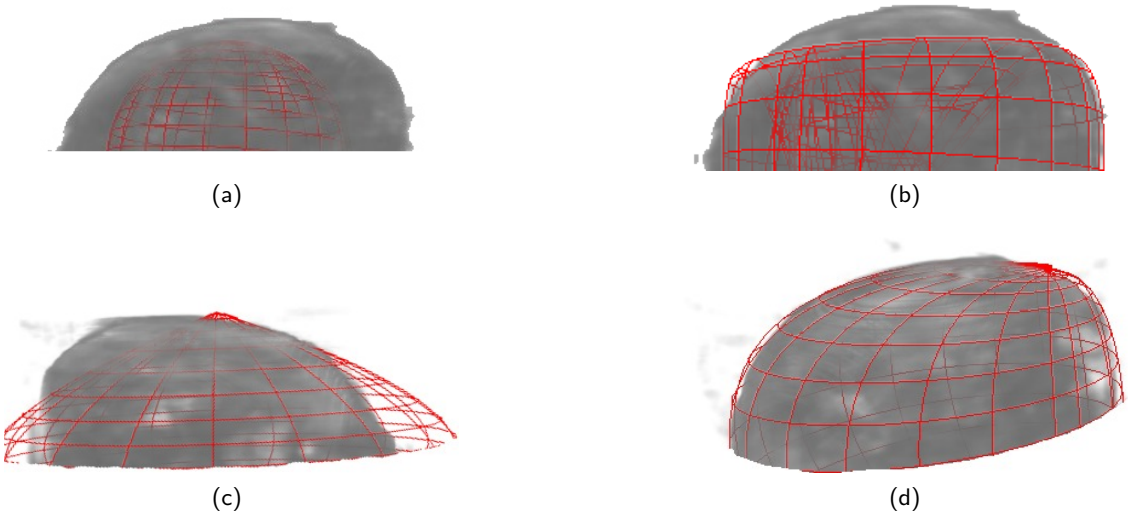

Figure 5. Breast segmentation using active contours with different initial shapes. (a) Initial spherical contour. (b) Segmentation using an initial spherical contour. (c) Initial conical contour. (d) Segmentation using an initial conical contour.

In Figure 6, we present more examples of segmentation using our strategy on clinical cases. We observe that the algorithm performs well despite the variety of breast shapes and sizes.

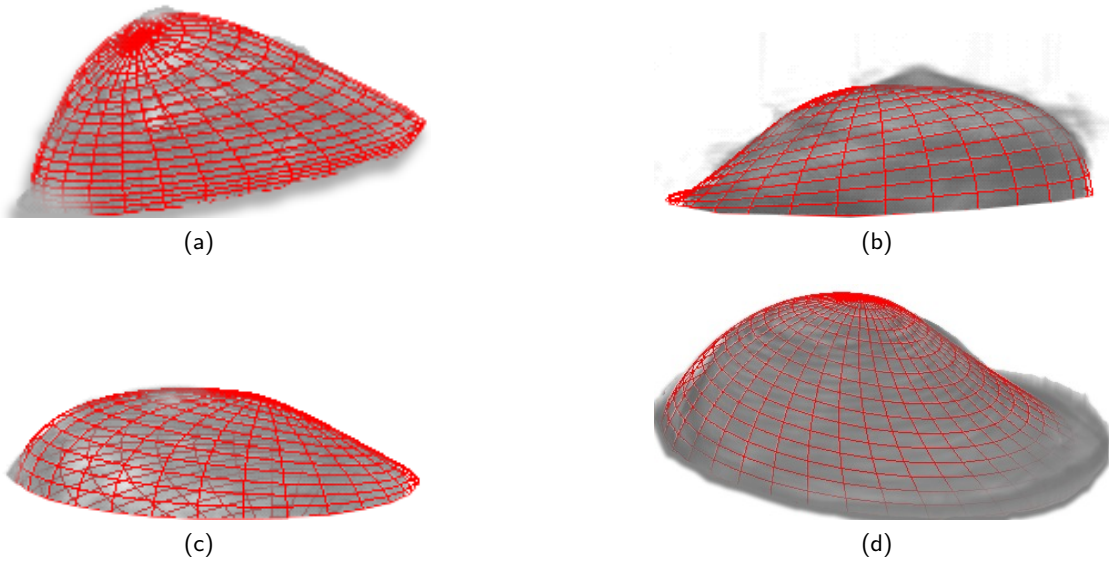

Figure 6. Breast segmentation using the proposed approach for different breast shapes and sizes.

5. CONCLUSIONS

We have investigated a segmentation problem where the boundary of a breast immersed in water needs to be estimated. We have presented a novel algorithm based on active contours that processes a stack of ultrasound tomography attenuation images in order to automatically detect the boundary of a breast immersed in water. The proposed method accurately detects the boundary of the breast without the need for user interaction. The method is fully automated, fast, and robust to artifacts that may arise from the ultrasound tomography reconstruction process. The effectiveness of our approach has been demonstrated on breast ultrasound images reconstructed from clinical data. Our current research efforts focus on improving the robustness of the algorithm on a larger set of clinical data.

REFERENCES

[1] V. Marmarelis, J. Jeong, D. Shin, and S. Do, "High-resolution 3-d imaging and tissue differentiation with transmission tomography," in *Acoustical Imaging*, M. Andr, I. Akiyama, M. Andre, W. Arnold, J. Bamber, V. Burov, N. Chubachi, K. Erikson, H. Ermert, M. Fink, W. Gan, B. Granz, J. Greenleaf, J. Hu, J. Jones, P. Khuri-Yakub, P. Laugier, H. Lee, S. Lees, V. Levin, R. Maev, L. Masotti, A. Nowicki, W. OBrien, M. Prasad, P. Rafter, D. Rouseff, J. Thijssen, B. Tittmann, P. Tortoli, A. Steen, R. Waag, and P. Wells, eds., *Acoustical Imaging* **28**, pp. 195–206, Springer Netherlands, 2007.

[2] S. A. Johnson, D. T. Borup, J. W. Wiskin, F. Natterer, F. Wuebbling, Y. Zhang, and S. C. Olsen, "Apparatus and method for imaging with wavefields using inverse scattering techniques," 1999.

[3] H. Gemmeke and N. Ruiter, "3d ultrasound computer tomography for medical imaging," *Nuclear Instruments and Methods in Physics Research Section A: Accelerators, Spectrometers, Detectors and Associated Equipment* **580**(2), pp. 1057 – 1065, 2007.

[4] N. V. Ruiter, G. Göbel, L. Berger, M. Zapf, and H. Gemmeke, "Realization of an optimized 3D USCT," in *SPIE*, **7968**, Mar. 2011.

[5] M. P. Andre, H. S. Janee, P. J. Martin, G. P. Otto, B. A. Spivey, and D. A. Palmer, "High-speed data acquisition in a diffraction tomography system employing large-scale toroidal arrays," *International Journal of Imaging Systems and Technology* **8**(1), pp. 137–147, 1997.

[6] N. Duric, P. Littrup, L. Poulo, A. Babkin, R. Pevzner, E. Holsapple, O. Rama, and C. Glide, "Detection of breast cancer with ultrasound tomography: First results with the Computed Ultrasound Risk Evaluation (CURE) prototype," *Med. Phys.* **34**, pp. 773–785, Feb. 2007.

[7] C. Glide-Hurst, N. Duric, and P. Littrup, "Volumetric breast density evaluation from ultrasound tomography images," *Medical Physics* **35**(9), pp. 3988–3997, 2008.

[8] R. Delgado-Gonzalo, N. Chenouard, and M. Unser, "Fast parametric snakes for 3d microscopy," in *2012 9th IEEE International Symposium on Biomedical Imaging (ISBI)*, pp. 852–855, 2012.

[9] R. Delgado-Gonzalo, N. Chenouard, and M. Unser, "Spline-based deforming ellipsoids for interactive 3d bioimage segmentation," *IEEE Transactions on Image Processing* **22**(10), pp. 3926–3940, 2013.

[10] R. Delgado Gonzalo, *Segmentation and Tracking in High-Throughput Bioimaging*. PhD thesis, STI, 2013.

[11] C. Xu and J. L. Prince, "Snakes, shapes, and gradient vector flow," *IEEE Transactions on Image Processing* **7**(3), pp. 359–369, 1998.

[12] M. Gebhard, J. Mattes, and R. Eils, "An active contour model for segmentation based on cubic B-splines and gradient vector flow," in *Medical Image Computing and Computer-Assisted Intervention*, W. J. Niessen and M. A. Viergever, eds., *Lecture Notes in Computer Science* **2208**, pp. 1373–1375, Springer Berlin Heidelberg, 2001.

[13] K. Zhang, L. Zhang, H. Song, and W. Zhou, "Active contours with selective local or global segmentation: A new formulation and level set method," *Image and Vision Computing* **28**, pp. 668–676, Apr. 2010.